BJR
© 2019 The Authors. Published by the British Institute of Radiology
https://doi.org/10.1259/bjr.20180505

Received: 04 June 2018 | Revised: 10 October 2018 | Accepted: 26 October 2018

Cite this article as:
Das IJ, McGee KP, Tyagi N, Wang H. Role and future of MRI in radiation oncology. *Br J Radiol* 2019; **91**: 20180505.

REVIEW ARTICLE

Role and future of MRI in radiation oncology

[1]INDRA J DAS, PhD, FACR, FASTRO, [2]KIARAN P MCGEE, PhD, FAAPM, [3]NEELAM TYAGI, PhD and [1]HESHENG WANG, PhD

[1]Department of Radiation Oncology, NYU Langone Medical Center, New York, NY, USA
[2]Department of Radiology, Mayo Clinic, Rochester, MN, USA
[3]Department of Medical Physics, Memorial Sloan-Kettering Cancer Center, New York, NY, USA

Address correspondence to: Prof Indra J Das
E-mail: *indrajdas@gmail.com*

ABSTRACT

Technical innovations and developments in areas such as disease localization, dose calculation algorithms, motion management and dose delivery technologies have revolutionized radiation therapy resulting in improved patient care with superior outcomes. A consequence of the ability to design and accurately deliver complex radiation fields is the need for improved target visualization through imaging. While CT imaging has been the standard of care for more than three decades, the superior soft tissue contrast afforded by MR has resulted in the adoption of this technology in radiation therapy. With the development of real time MR imaging techniques, the problem of real time motion management is enticing. Currently, the integration of an MR imaging and megavoltage radiation therapy treatment delivery system (MR-linac or MRL) is a reality that has the potential to provide improved target localization and real time motion management during treatment. Higher magnetic field strengths provide improved image quality potentially providing the backbone for future work related to image texture analysis—a field known as Radiomics—thereby providing meaningful information on the selection of future patients for radiation dose escalation, motion-managed treatment techniques and ultimately better patient care. On-going advances in MRL technologies promise improved real time soft tissue visualization, treatment margin reductions, beam optimization, inhomogeneity corrected dose calculation, fast multileaf collimators and volumetric arc radiation therapy. This review article provides rationale, advantages and disadvantages as well as ideas for future research in MRI related to radiation therapy mainly in adoption of MRL.

INTRODUCTION

Radiation therapy is used in nearly 60% of all cancer patients for the management of care either in curative intent or terminal and palliative approaches.[1] For many disease sites such as the breast, prostate, lung, and head-and-neck tumours, radiation has become an integral part of combined multimodality treatment approaches. For curative approaches, the goal of radiation therapy is to maximize the dose to the target volume while simultaneously minimizing the dose to adjacent organs at risk (OAR). In other words, adoption of ALAP (as low-dose as possible) for OAR should yield less toxicity while allowing possible dose escalation to target thereby resulting in improved patient care. To achieve the goal, the target volume needs to be precisely delineated. This is achieved through multimodality imaging including but not limited to CT, PET, and MRI. Additionally, as the tumour is usually not static and moves along with organ motion, the simplest approach to address this issue is to provide a wide margin around the target to create a planning target volume (PTV). However, a wide margin around the target has serious (cubic factor) implications both in terms of irradiating OAR and normal tissues.[2] Thus image-guided radiation therapy (IGRT) and adaptive therapy have been developed to specifically address these issues.[3]

Historically in radiation therapy, MR and CT images have provided complementary information. CT data provides image information with high spatial fidelity and direct correlation between electron density and of Hounsfield numbers that is related to the radiation dose.[4] However, CT provides relatively poor soft tissue discrimination and is prone to artefacts, particularly in the presence of high atomic number materials such as metallic prosthesis. On the other hand, MRI images provide superior visualization of soft tissues as well as a range of tissue contrasts that CT is unable to match. To obtain the benefits of both modalities in the treatment planning process, CT and MR images are fused, providing hybrid image data sets as illustrated in Figure 1. Figure 1a shows the case of a brain tumour CT-MR fusion. The lesion treated with stereotactic radiosurgery (SRS) is inconspicuous on CT but is clearly visible on post contrast spoiled gradient recalled (SPGR) gradient echo and T_1-weighted spin echo images. Similarly Figure 1b shows a head and neck CT-MR fusion with metal artefact. The patient has a significant dental amalgam that

Figure 1. (a) A small brain lesion invisible in CT images, but can be clearly visible in MR images, (b) another patient with dental filling where CT images are difficult to provide volume delineation. The MR images can provide structural information. The CT-MR fusion is used for target and normal tissue delineation.

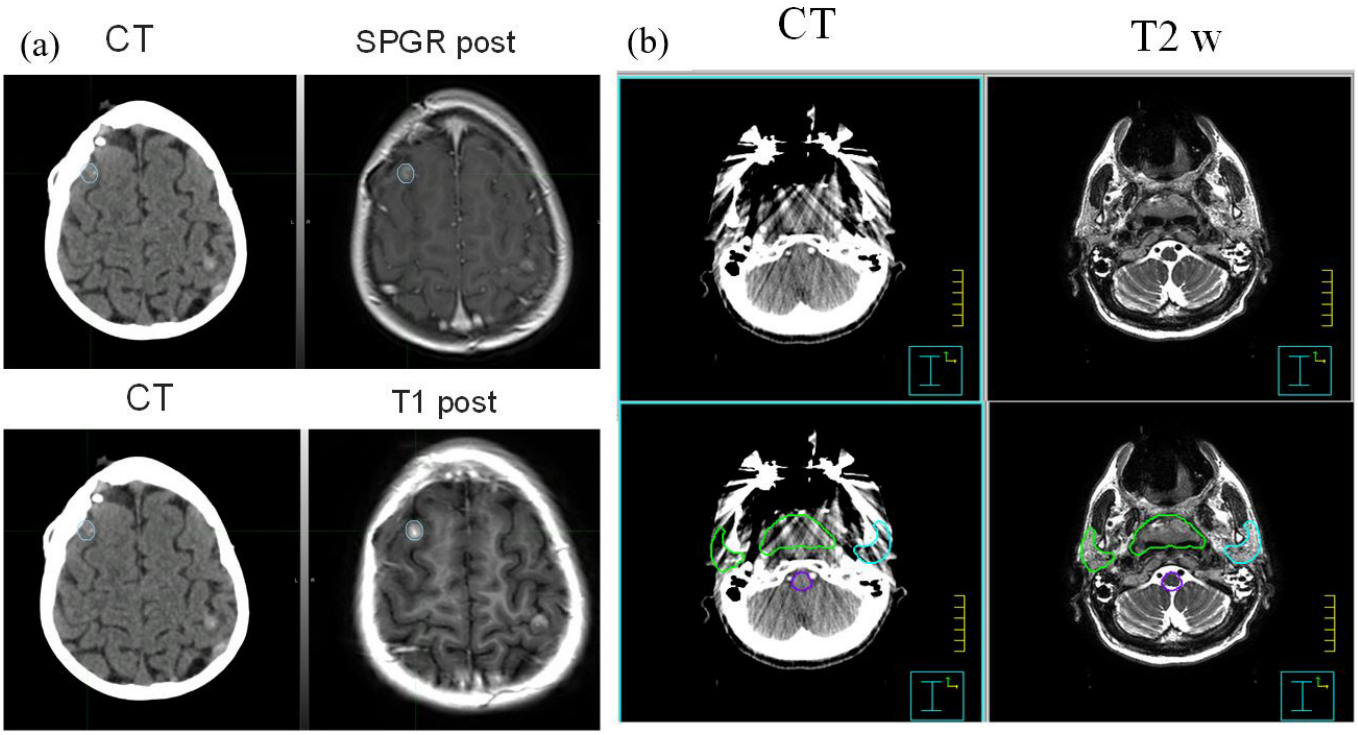

resulted in significant streaking. Even though the corresponding MRI images show susceptibility induced signal loss, the signal loss does not spill over to the target and normal structures and is very helpful for contouring these structures.

The role of MRI for soft tissue visualization and discrimination is so convincing that a number of centres (Sweden and Canada) have installed a dedicated MRI unit adjacent to or within the treatment room either in a fixed configuration or on rails very similar to the CT-on rails concept. Early MRI installations in radiation oncology were used primarily for simulation of the prostate and head and neck tumours on a relatively low magnetic field (0.23 T).[5] The past decade has seen the development of 1.0 T, 1.5 T and now 3 T MR simulators that are dedicated for radiotherapy simulation.[6] These dedicated MR simulators have generated not only CT-MR based simulation workflows but also MR-only simulation and planning workflows with the help of synthetic CT (sCT) data generated directly from MR images.[7–12]

Currently MR-simulation is not integrated process and as such has resulted in an inherent time lag between simulation, patient transport and finally treatment, even though both systems may be within close proximity to one another.[13] This will be true for CT-simulation also if scanner is not located in the department. With advent of CT-PET and MRI-PET, it became apparent that data could be acquired simultaneously or sequentially within a single coordinate system, initiating the idea of integrating MR imaging and megavoltage therapy systems into a single unit and has resulted in the development and marketing of an MRI based integrated imaging and treatment systems both in Europe and USA. The Utrecht group has been actively working on this project since 2002 that has culminated in Elekta Unity system (Elekta AB, Stochholm, Swededn).[14] In the USA, the ViewRay MRIdian system (Oakwood OH) was introduced with a Co-60 beam.[15,16] These systems are meant to provide an integrated MRL device for simultaneous MRI imaging and advanced treatment with adaptive therapy.

Various groups have also received funding to produce integrated systems with varying magnetic strengths.[14,17–20] Current systems in use include 0.35 T, 0.5 T, 1.0 T, and 1.5 T for ViewRay, Alberta group, Sydney group and Elekta system, respectively. Various approaches have been proposed with functional or prototype units. For example, first in class was the ViewRay unit based on 0.35 T magnet and three Co-60 heads placed at a circular gantry with 90 cm source to axis distance, but newer system has replaced the Co-60 sources with a 6 MV linear accelerator. The Elekta Unity is 1.5 T magnet with advanced imaging capabilities and uses 6 MV linear accelerator.[21] The Canadian system at University of Alberta, Aurora-RT uses a 0.5 T magnet with a 6 MV linear accelerator placed in central opening of the magnet.[19,20] The Australian Consortium is working on a system that will use a 1.0 T magnet.[18] Images of these systems are shown in Figure 2. The specification and functioning of these systems can be viewed from various references.[14,15,17–20]

The availability of MR simulators within radiotherapy departments has increased the use of MR images as both primary and secondary imaging modalities. With the recent availability of MRL systems, advanced treatments such as intensity modulated

Figure 2. (a) ViewRay MRIdian system, (b) Elekta 1.5 T MRI-Linac, (c) Alberta's Aurora RT system and (d) Australian (Sydney) MRI System, image courtesy of Paul Keall and Brad Oburn.

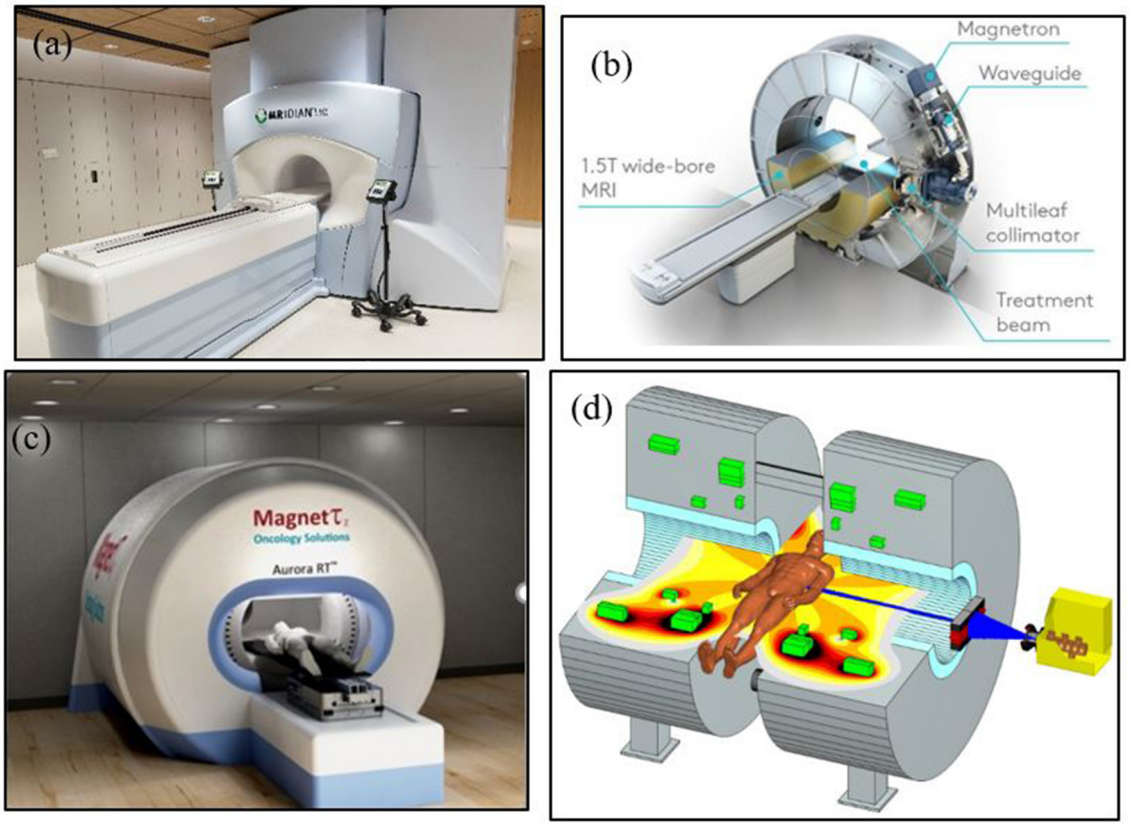

radiotherapy/volumetric modulated arc therapy (IMRT/VMAT) and stereotactic body radiation therapy (SBRT) or stereotactic ablative radiotherapy (SABR) are likely to be developed and translated into clinical practice. At the time of publication of this article, it is too early to speculate the future of MRL.

USE OF MR FOR RADIOTHERAPY: HISTORICAL REVIEW

Adaptation and clinical integration of MR for radiation therapy treatment simulation has been slow. The reasons for this are several fold including; technical limitations of the equipment, access issues related to the physical locations of these systems within radiology departments and therefore physically remote from radiation oncology, concerns regarding the spatial fidelity of the MR data and the lack of electron density information. By far the greatest contributor to this delay relates to the technical limitations imposed by early MR scanner designs. These limitations arose due to the fact that, from their outset, they were designed as diagnostic imaging instruments in which disease conspicuity was the first and foremost performance criterion. This was achieved by ensuring the patient was imaged in a neutral position within a rigid RF coil and not placed in an immobilization device in treatment position. The development of early high field systems (≥1.5 T) with bore diameters of 50–60 cm further restricted in treatment position imaging while in those situations in which the patient could be imaged in treatment position, space limitations within the bore routinely prohibited the use of dedicated RF coils, most notably surface coil arrays resulting in imaging being performed using the whole body transmit receiver RF coil. The consequence of which was a degradation of image quality due to a reduction in signal-to-noise ratio (SNR) within the image.

The development of open MR scanners provided an early opportunity to address many of the aforementioned technical challenges. The first reported case of the use of an open MR scanner for radiation therapy treatment simulation was by Mizowaki et al[22] in 1996. In 2002, Mah and colleagues[5] reported on the integration of a 0.23 T open system into their radiation oncology department specifically for MR treatment simulation. The system consisted of two 1 meter diameter cylindrical magnets separated by 47 cm. While the anteroposterior separation of the magnet poles was similar to so-called closed bore systems, the use of separate magnet poles provided 360° of unrestricted access in the plane orthogonal to the field direction thereby facilitating imaging in treatment position using MR compatible patient immobilization. While the technical performance of this system was inferior to contemporary high field systems, the location and installation of this and other systems directly into radiation oncology departments was an important clinical proof of concept and milestone. More recently, Glide-Hurst and colleagues[6] have reported on the development of a 1.0 T MR scanner dedicated for radiation therapy treatment simulation.

While open MR systems addressed a critical clinical challenge in MR simulation—the ability to image in treatment position—these

systems were compromised in terms of SNR and overall performance when compared to their closed bore high field counterparts. The introduction of so-called wide bore systems in which the largest bore dimension equalled 70 cm addressed the most significant limitation of these systems by dramatically increasing the population of patients who could be imaged in their immobilization systems in treatment position while simultaneously providing access to advanced imaging techniques such a functional, rapid and parallel imaging. As a consequence, institutions and MR scanner manufacturers have focused on these systems as the primary platform for MR simulation.

THE USE OF MR IN RADIOTHERAPY: EXISTING CHALLENGES

Significant challenges remain to be addressed in regards to the development of MR for radiation therapy.[23] Due to the relatively long acquisition times of MR data in general and 3D MR data specifically, motion related artifacts and motion management remain problematic, particularly so when imaging organs within the abdomen and chest.[24] The 4D MR imaging allows for the acquisition of data acquired at multiple time points across the respiratory cycle is an active area of research that could be helpful in managing target motion during beam delivery. Another challenge remains the ability to accurately image cortical bone and to derive electron density information from MR data. Zero echo time (ZTE) and ultrashort echo time (UTE) are two MR methods that provide promise to address these issues and will be discussed below. Finally, RF coil designs remain sub optimal for many MR simulation applications. The development of flexible multiple element phased array coils have proven to be superior when compared to rigid coils due to their ability to more closely conform to an individual's positioning and body habitus. Despite their flexibility, they remain bulky and in general are only draped over the patient and doing so do not accurately follow a given patient's contour. Recent developments in RF coil technology show promise in this regard. Highly flexible, low profile so-called 'AIR' coils (GE Healthcare, Waukesha, WI) have been demonstrated to address many of the existing limitations of conventional coils encountered in radiation therapy MR simulation.[25] Due to their developmental nature, it remains to be seen if these RF coil systems will be adopted by the MR community.

MR BASED TREATMENT PLANNING CHALLENGES

Spatial distortions and artefact

Ensuring the spatial fidelity of the MR data set is essential for precision radiation therapy and early reports regarding spatial distortion of MR data were as large as tens of millimetres.[22,26] It is important to note that these data were acquired on low field (0.2 T) systems and reported as early as 1996.[22] Recently Wegand et al[27] described the results of 12 studies investigating spatial distortion in MR and reported that spatial distortion was of the order of several millimetres with five studies quantifying maximum spatial distortion to be less than 2 mm. In general, spatial distortion will increase with increasing distance from the isocentre of the MR scanner and as such, large field of view or off isocentre imaging will be most susceptible to image distortion.

Spatial distortion is generally considered to be comprised of both system dependent and patient dependent sources.[27] System dependent effects are due to system imperfections such as gradient non-linearity, inhomogeneities of the main magnetic field (ΔB_0), eddy currents and concomitant fields and inhomogeneity of the radiofrequency (RF) pulse profile. Patient dependent sources are generally considered to arise from magnetic susceptibility differences of tissues and implanted devices such as metal implants and chemical shift effects, both of which distort the main magnetic field.

Much work has been done to reduce system dependent distortions. Because gradient field non-linearity arises from physical imperfections in the construction of the gradient coils, it can be effectively modelled and corrected for. Gradient induced distortion is commonly characterized using spherical harmonics as the basic function[28] with spatial errors being characterized by the sum of Legendre polynomials of increasing order. The higher the order of the polynomial, the more accurate the model of the distortion field.[28] The high order modelling of the gradient induced distortion means that correction of these spatial errors is nonlinear and is consequently referred to as gradient warping (Gradwarp). In general, MR scanner manufacturers provide Gradwarp distortion correction in both 2D and 3D depending upon whether planar or volumetric data is acquired. While the effects of inhomogeneity of the B_0 field can be quantified, quantitative ΔB_0-distortion correction methods are less frequently employed. Typically, B_0 shimming is performed in which both first and second-order corrections using the spatial encoding and other dedicated coils are used to correct for ΔB_0 within the prescribed imaging volume at the time of pre-scanning. Importantly, it can be shown that the magnitude of both types of distortion are inversely proportional to the amplitude of the spatial encoding gradient in the readout direction for conventional acquisition techniques.[27] Hence, those sequences that use larger gradient amplitude in the readout direction will be less susceptible to distortion arising from these sources.

Distortion arising from susceptibility differences and chemical shift effects are patient specific and therefore a general solution to ameliorate their effects does not exist. Distortions resulting from susceptibility differences between tissue and air or between tissue and foreign active or passive implanted devices is dependent upon susceptibility differences, the geometry of the implant as well as it's orientation within the main magnetic field.[29] Susceptibility induced artifacts scale with the main magnetic field and are inversely proportional to the amplitude of the readout gradient. Hence, imaging at lower field strengths (1.5 *vs* 3.0 T) or increasing the bandwidth of the imaging sequence (increased readout gradient) are two strategies for reducing this effect. Artifacts arising from susceptibility differences between tissue and foreign metal can be minimized using a variety of metal artefact reduction techniques. However, the amount of artefact reduction is related to the composition, amount and orientation of the metal. In the absence of dedicated pulse sequences for metal artefact reduction, spin echo based sequences are more immune to distortion compared to gradient echo based sequences. Chemical shift artifacts arise from a shift in the Larmor frequency between

fat and water and are manifested as either a physical miss-mapping of fat relative to water (chemical shift of the first kind) or a cancellation of the MR signal within voxels that contain both fat and water (chemical shift of the second kind).[30] As with susceptibility artifacts, these effects scale with field strength. Chemical shift of the first kind can be minimized by imaging at a lower field strength or increasing the bandwidth of the imaging sequence. Chemical shift of the second kind can be minimized by judicious choice of imaging echo time.

Electron return effect

Radiation dose in a patient is related to the secondary electrons produced by photon interactions arising from photo-electric, Compton and pair production process. Each of which is dependent on beam energy and characteristics of the medium (atomic number and density). The computation is generally performed on CT data which in turns provide electron density needed for the dose computation. The development of MR-linacs has resulted in the violation of the charged particle transport and therefore the need for modelling of charge particle motion within a large magnetic field which is critically important for dosimetry.[31] Referred to as the electron return effect, MRL dosimetry and treatment planning must account for charged particle path deviation due to the Lorentz force. Various approaches to overcome this is being proposed in various system with some success.

Target volume delineation

Delineation of the treatment target and OAR are a prerequisite for a treatment planning and are acquired primarily from CT data. In general there are no universal guidelines for volume delineation except in a few disease sites, thus significant variability exists. In the absence of guidelines, the accuracy of target delineation is determined by image quality as well as the expertise and training of the clinician. Multiple publications have highlighted this variability in several treatment sites including the breast, lung, prostate, head and neck and others.[32–37] The dose-volume histogram (DVH), originally developed during the 3DCRT era as a treatment planning optimization tool is now universally used but its accuracy depends on volume estimation that varies with slice thickness and treatment planning system.[2] While volume delineation can be augmented by multimodality imaging (CT, PET, MRI) it has been noted that even with such approaches the process is in general sub optimal.[38] Several of the difficulties related to target and OAR contouring and volume delineation are discussed below.

MR as secondary imaging modality

As early as 1998, Ramsey et al[39] reported work flows, and general usage of MRI in radiation oncology. To date, the utility of MR as a secondary imaging modality is without question, particularly in regards to the reduction of inter observer variability in contouring as compared to CT across multiple anatomical sites.[32,38,40] However, errors introduced by mis-registration of CT and MR images have shown to be significant due to changes in the shape and location of the soft tissues between imaging sessions as a result of surgery, chemotherapy or due to the fact that MRI has been acquired not in treatment position. In case of SBRT treatments, this can compromise tumour control because of the steep dose gradient between tumour and OAR. The introduction of MRL and MR simulators equipped with an indexed flat table top, MR compatible immobilization, coil bridge support and lasers for alignment and marking, these registration uncertainties can be minimized.

Figure 3a,b are an example of gynaecological and prostate MR simulation cases. For gynaecological case, the GTV boundary is more clearly visible on the MR as compared to CT. The prostate patient with bilateral hip implant shows prostate and rectal spacer more clearly on the MR as compared to CT. Additionally as shown in Figure 1b, the impact of image artifacts can be minimized in some cases with the use of MRI.

MR-ONLY APPROCHES

Synthetic CT and DRR generation

Even though segmentation errors introduced by miss-registration between CT and MR could be minimized with the introduction of an MR only pathway, disease and/or treatment induced changes in target and normal tissue volumes across different imaging sessions is still a concern. Figure 4 shows a typical MR-only planning approach. In addition to minimizing segmentation errors, an MR only workflow improves efficiency and convenience to the patient by reducing the number of imaging sessions. A crucial requirement for MR-only simulation and planning is the ability to perform dose calculations based on MR images only. To address the challenge of the absence of electron density information from MR-only simulation, research is currently underway to develop so-called "pseudo CT; sCT" for dose calculation. Recent growth of MR simulators in radiation oncology departments has resulted in rapid growth of sCT development for MR-only planning workflows for different anatomical sites for accurate dose calculation. These methods can also be extended to MR-linac, where a MR-only workflow maybe more suitable for daily online adaptation. Although, both dosimetric and geometric accuracy (accuracy of DRRs and CBCT matching) of sCT is important for a linac-based MR-only workflow, for an integrated MRL system where online image guidance is MR-based, volumetric matching of MR images is more crucial than DRR-based matching. In this scenario, evaluating the dosimetric accuracy of sCT, especially in the presence of a magnetic field, is more relevant than geometric accuracy.

Bulk density assignment-based methods for sCT

These methods are the simplest sCT-based methods and rely on manual contouring of bones and other relevant tissues such as soft-tissues, lung, air, etc and assigning a bulk electron density to the segmented structures. The method has shown dose calculation accuracy within 2–3% to the standard CT-based photon plans for brain,[43] head and neck,[44] prostate,[44,45] lung and pancreas.[46] The limitation of this method is manual contouring of structures, such as bones, which is not practical for routine use and assigning appropriate bulk electron density value. In the future, development of auto-segmentation of bones on MR images may overcome the challenge of manual contouring of this relevant structure.

Figure 3. MR simulation example cases: (a) Axial CT + MR fusion of a Gynaecological case. GTV boundary, red colour (bottom panel) is clearly visible on the T_2w MRI acquired in treatment position, (b) Axial CT + MR fusion of a prostate patient with bilateral hip implants. Prostate and rectal spacer is clearly visible on the axial T_2w MRI as compared to CT (arrow).

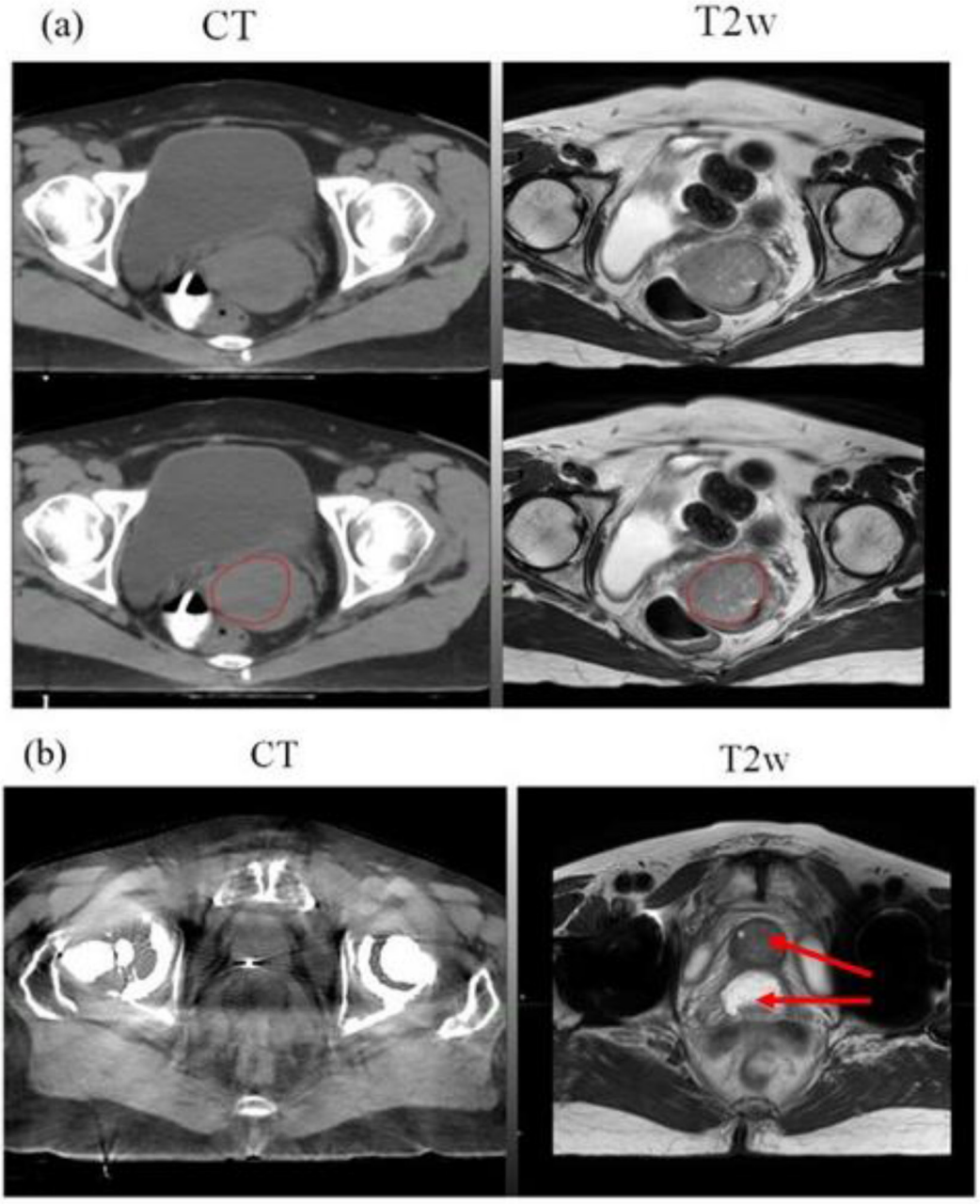

These methods are the simplest sCT-based methods and have shown dose calculation accuracy within 2–3% to the standard CT-based photon plans for brain,[43] head and neck,[44] prostate,[44] lung and pancreas.[46] Manual contouring of structures, such as bones makes it impractical for routine use. In the future, development of auto-segmentation of bones on MR images may overcome the challenge of manual contouring of this relevant structure. Once validated, auto-segmentation based bulk density assignment methods maybe suitable for MR-only planning as well as online planning on the MRL.

Atlas-based methods

Atlas-based methods have been used to generate sCTs for brain,[47] head and neck,[48] and prostate[49] and have shown good dosimetric accuracy of less than 2%. These methods can also be used to propagate contours in addition to generating sCTs and are suitable for MR-only workflows on MRL. The main drawback of atlas-based method is that they are limited by the accuracy of deformable registration especially in situations where there is a large variation in patient anatomy as compared to the atlas subjects. In addition, the individual atlas may need to be

Figure 4. MR only approach to patient treatment. (a) T_1/T_2 image acquired on a flat table top used for contouring, (b) sCT generation, (c) treatment planning (d) two images (bone and soft tissue) of sCT DRR for treatment verification. Similar approaches and detailed DRR images are also provided by several other investigators.[41,42]

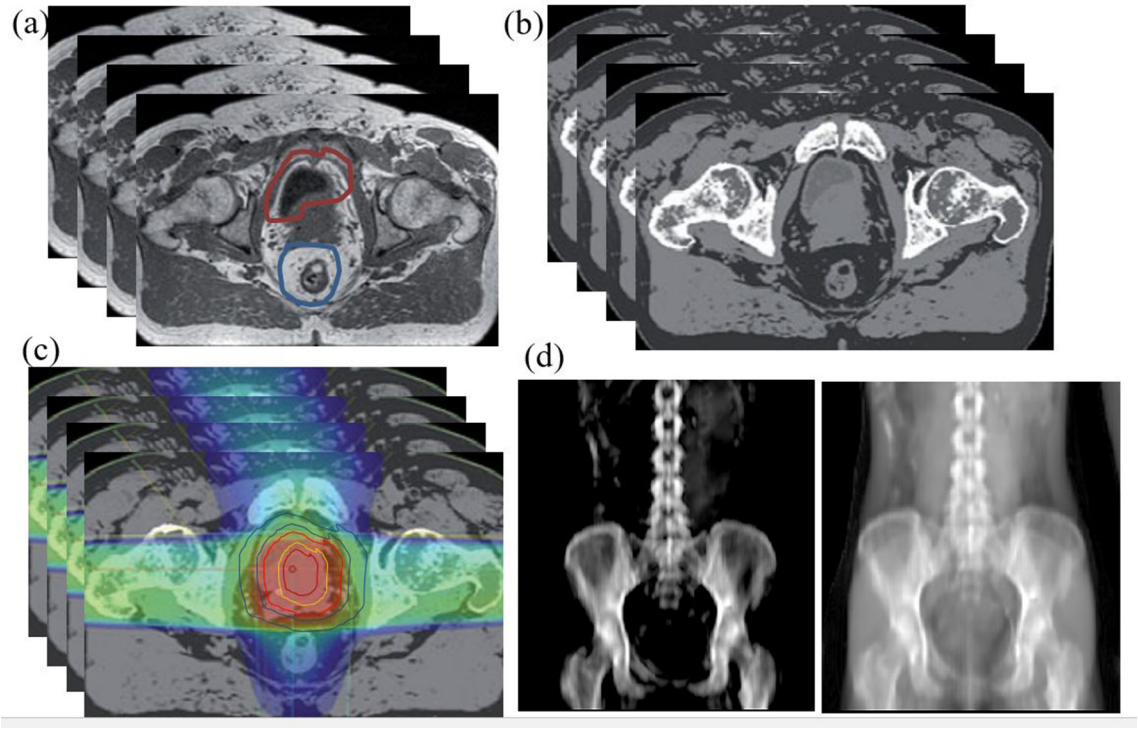

developed for each treatment site with an optimal number of atlases in each site. Even for a streamlined MR-only workflow, it would be ideal to generate synthetic CT in real-time before the patient has left the simulation appointment so that a backup plan can be initiated if any issues are detected with the synthetic CT generation.

Other methods

Recently, the use of standard MR images along with deep learning-based convolution neural network methods are being developed for sCT generation and have shown good accuracy in the brain[9] and prostate.[50] Although deep learning based methods take longer to train, they are extremely fast (order of seconds) in generating the sCT and have the potential to classify bone without the use of specialized sequences such as ultrashort echo or UTE. These deep learning based models can be trained based on paired or unpaired[51] MR-CT images and have great potential to be used in a MR-only workflow or online MR guided setting.

Commercial solutions

There are several commercial sCT software solutions that are available for MR-only planning for prostate for clinical use. Such automated approaches maybe more clinically useful for MRI based treatments. One of them is a classification-based method called MRCAT (Philips Healthcare NA, Cleveland OH) or MR for Calculating Attenuation, which is currently limited to a Philips MR scanner. The method uses a Dixon based MR sequence along with a constrained bone model to generate sCT by assigning bulk HU for water, fat, and spongy and cortical bones. The method has been clinically implemented for MR-only planning for prostate[52] and has strong potential to be used on Elekta MR-linac systems. The other method (MRI planner; Spectronic Medical AB, Helsingborg, Sweden) is scanner independent and currently CE marked for clinical use in Europe.[53] Recently, Siemens have launched a sCT software that will be available shortly on a new sola MRI system. MRIplanner uses a statistical decomposition algorithm for generating sCT and has been evaluated for dosimetric accuracy within a multicentre/multivendor validation and shown accuracy to be within 1% of CT-based plans.[53] MRIplanner although scanner independent, may need to be evaluated for low-field-strength (0.35 T and 1.0 T) MRL systems.

Digitally reconstructed radiographs (DRR) generation

The transition to MR only treatment simulation and planning requires the use of DRRs or 3D verification using cone beam CT (CBCT) for treatment verification that rely only on MR data. The CT based simulated radiograph or projection images have been widely used in radiation therapy for several decades with their spatial fidelity and radiographic characteristics have been well characterized and understood. However, recently CBCT is being used frequently. Currently DRRs are generated in beam's eye view (BEV) from treatment planning systems that act as a reference image. These DRRs are then compared with pre-treatment images either from on-board imaging or portal images. The quality and fidelity of DRR is critical for the matching of pre-treatment images to set up patient with calculated shift for treatment. Thus, there is considerable interest in the characterization of MR-only DRRs both in terms of their spatial fidelity/accuracy and radiographic properties. Because MR-only DRRs are generated from MR data, spatial fidelity is determined by

the amount of distortion, the intrinsic resolution of the MR data and the accuracy of classification of the bones on sCT. With recent developments in sCT methodologies as described in the previous section, the quality and accuracy of DRRs are as good as those obtained from real CT. Kemppainen et al[41] have demonstrated that errors between MR-only DRRs and those generated from CT data within the prostate can be less than 1 mm when imaging the prostate. Based on the survey by Johnstone et al[42] which included multiple treatment sites and DRR methodologies, errors of no greater than 4 mm were reported. After systematic evaluation of MR based positional accuracy, few institutions are clinically using MR based DRRs for brain and prostate as part of their MR-only simulation and planning program.[8,48,54]

TREATMENT DELIVERY TECHNOLOGIES

Visualization of a target in radiation oncology has been challenging, especially during treatment. Kishan and Lee[55] recently noted that radiation therapy has been 'blind' to the target anatomy. The inability to visualize the target during treatment resulted in the development of various treatment imaging systems including cone beam CT and portal imaging to address this limitation. However, no X-ray based approaches have been able to provide the soft tissue contrast afforded by MR and has therefore spurned multinational research efforts to incorporate MR imaging into a radiation therapy treatment system. To date, several commercial and research systems are available or under development as described in detail by Pollard et al[56] including ViewRay system[15] which has replaced the threeCo fixed heads with a 6 MV linear accelerator and multi leaf collimator system. The MRL system developed by European consortium based on 1.5 T MR scanner, marketed by Elekta, is commercially known as the Unity system and described in detail in literature.[14,57,58]

Owing to ERE in magnetic field especially for higher field strength, Canadian group in Alberta designed magnetic field parallel to the beam axis with lower field strength (0.5 T) (Figure 1c).[19,20] Australian consortium is also working on a prototype with 1.0 T magnetic field MRI-Linac as shown in Figure 1d.[18]

TREATMENT DATA ASSESSMENT

Quantitative MR

MR imaging systems, including the imaging systems of MRLs are not measurement devices. This is because they have historically; identification and quantification of sources of bias and variance has not been performed, standardized acquisition and analysis techniques that are vendor agnostic are absent, and standardized quality control programs and phantoms that are traceable to national and international standards do not exist. This therefore represents a challenge for the integration of MR into radiation therapy for therapy response assessment which imposes the strict criteria of quantification of disease stage and type, its precise spatial extent, and response to therapy. The inability to provide precise quantitative information has the further potential to result in treatment decisions that are neither precise nor accurate. Efforts are in the way to make standardized quantification of the biomarkers as described by Pollard et al.[56]

MR for treatment response

The goal of radiation therapy is to effectively eradicate tumours while minimizing damage to normal tissues. The standard approach in determining tumour response uses the Response Evaluation Criteria in Solid Tumours (RECIST). It may take weeks for RECIST criteria to suggest success or failure of a treatment based on gross change of tumour size. Similarly, assessment of normal tissue effect based on adverse events could miss the time window for treatment adjustment to achieve better therapeutic outcome. Advances in MR imaging allow noninvasive assessment of morphological, biological and functional process in tissue, and, therefore, may provide tools for early assessment and prediction of tumour and normal tissue responses to irradiation. One such example based on longitudinal change in T_2 weighted MR images of a rectal cancer patient undergoing neoadjuvant chemoradiation treatment are shown in Figure 5. A good responder and a poor responder based on pathological response has been shown using longitudinal morphological information where persistent tumour burden is visually apparent for a poor responder. Imaging and pathological information combined from a larger patient cohort can be used to develop a predictive model. Figure 6 provides an example where image texture analysis features were used to indicate image correlation and outcome in nasopharyngeal tumours.[59]

Assessment of tumour response

Dynamic-contrast enhanced (DCE)-MRI characterizes tissue vasculature and has been proved clinically useful for tumour diagnosis and treatment assessment.[54] Perfusion and permeability parameters derived from DCE-MRI are consistently linked with tumour response to radiation on various anatomies including brain,[60] head and neck,[61] breast,[62] liver,[63] prostate and pelvis.[64,65] While DCE-MRI in the lung is susceptible to respiration motion, a prospective study showed DCE-MRI perfusion parameters predicted treatment response for non-small cell lung cancer (NSCLC) after chemo-radiotherapy.[66] Discriminating necrosis and tumour recurrence after RT is a long-time challenge in treatment of brain tumour. Using the transfer constant K_{trans} derived from DCE-MRI, Bisdas et al[67] achieved 100% sensitivity and 83% specificity for detecting recurrent gliomas from radiation necrosis.

Diffusion-weighted MRI (DWI) generates contrasts based on random Brownian motion of water molecules in biological tissues. The apparent diffusion coefficient (ADC) calculated from DWI quantifies tissue cellularity and has shown potentials for monitoring cell apoptosis, tumour lysis and necrosis.[68] However, DWI for brain tumours is often confounded by surrounding edema and necrosis. By spatially differentiating low and high ADCs, a diffusion abnormality index may provide a better metric in predicting response of brain metastases to whole brain irradiation.[69] DWI acquired with a high b-value identified hypercellular components in glioblastomas and may surrogate progression-free survival after radiation.[70] The potentials of ADC change in assessing tumour response to RT have also been demonstrated for RT of head and neck cancer,[71] prostate cancer etc.[72]

Figure 5. Morphological assessment of tumour burden based on longitudinal T_2 weighted MRI of rectal cancer patients undergoing neoadjuvant chemoradiation treatment. Please note changes in tumor burden over time with tumour location indicated by the arrow.

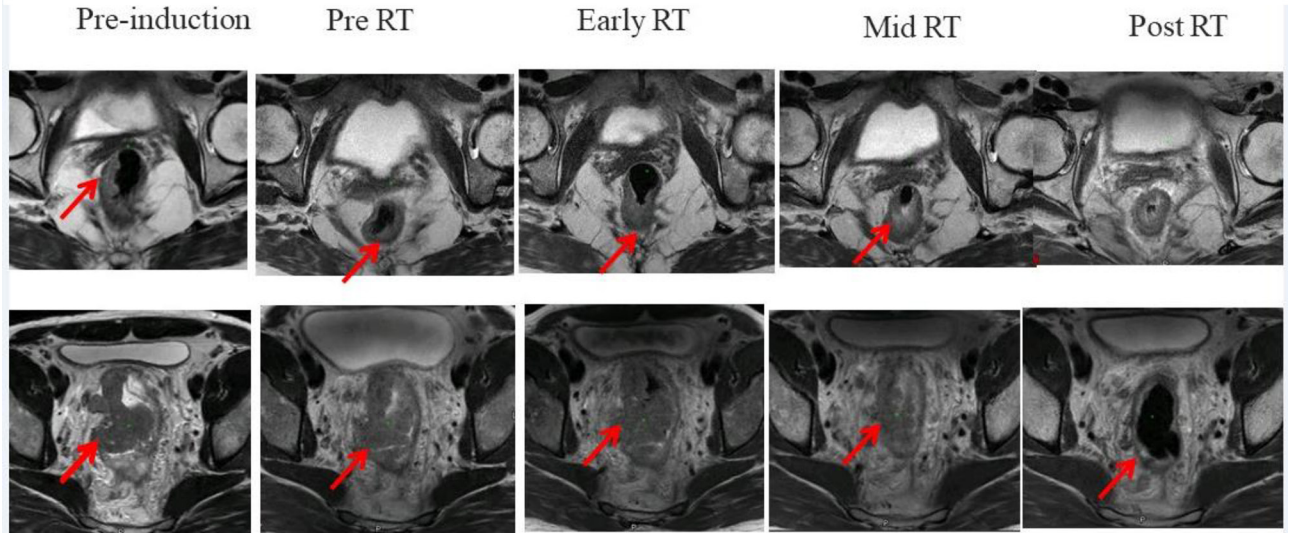

Assessment of normal tissue effect

Increased radiation dose for improved tumour control is limited by possible normal tissue injury. There are clear differences among patients regarding normal tissue radio-sensitivity; however, standard radiotherapy has been designed with "one dose fitting all" dose schedules to have no more than 5–10% of patients developing severe side-effects. Several studies have utilized MR functional imaging for early prediction of organ injury toward the goal of adaptive treatment and personalized medicine.

Radiation injury in the brain is often defined clinically by the development of neurocognitive dysfunction. By correlating with neuropsychological test results, the change of vascular volumes and blood-brain barrier permeability derived from DCE MRI

Figure 6. Schema for the image post-processing on contrast-enhanced T_1 and T_2 images. The tumour areas were contoured on all MRI slices. Radiomics features are extracted that is correlative with clinical data for survival prediction. Adopted from Ouyang et al[59] with open access source.

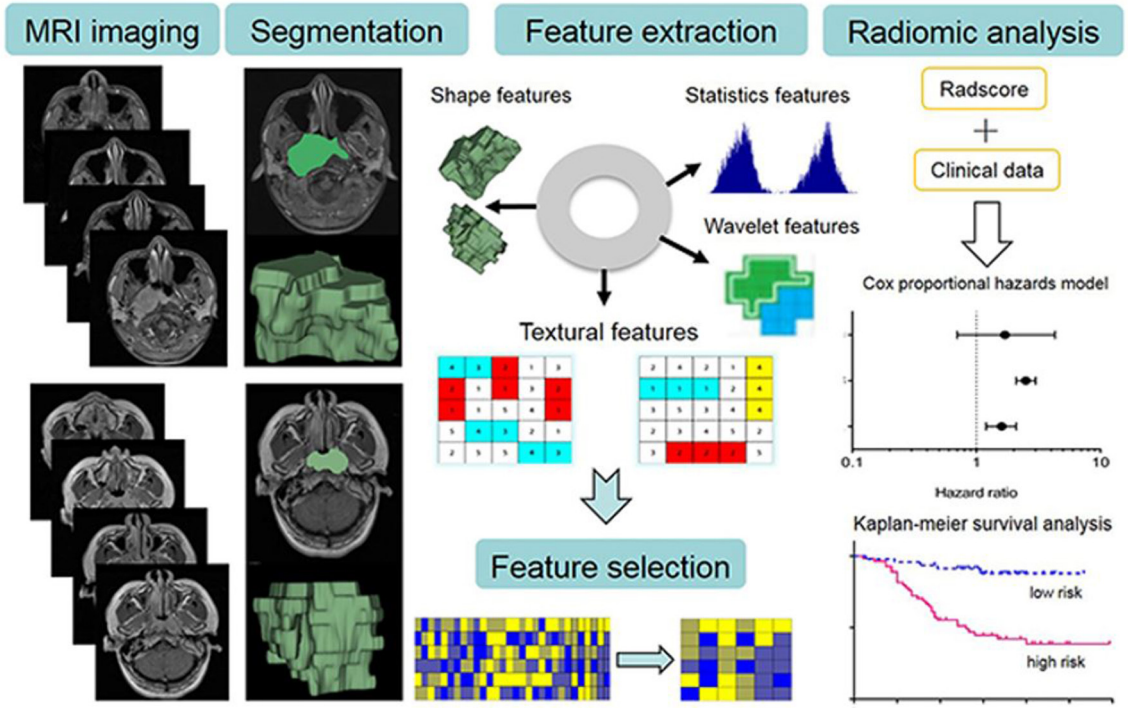

were predictive of delayed alternations in verbal learning and total recall after partial brain RT.[73] Diffusion tensor imaging (DTI) provides magnitude, anisotropy and orientation of diffusion of water molecules. Early diffusivity changes assessed by DTI were associated with late delayed cognitive decline.[74] A DTI white matter (WM) tractography analysis suggested the dose to elongated WM associated with WM post-treatment damage.[75] Radiation necrosis is a severe adverse effect of brain radiotherapy. DTI radial diffusivity may provide an early prediction for delayed radiation necrosis.[76] Radiation-induced liver disease (RILD) is a major factor that limits dose escalation for intrahepatic cancer. As the portal vein supplies approximately 75% of blood flow to the liver, portal venous perfusion derived from liver DCE-MRI could be a surrogate of spatial distribution of liver function in RT.[77] Relating the perfusion to function probability, a local and global function model was proposed to assess individual and regional dose-response of hepatic function.[78] Incorporation of the portal venous perfusion information into conventional NTCP modelling could improve estimation of the risk of liver injury compared with using dose only.[79]

MR habitats and radiomics

Tumours are not uniform within a volume, which may be responsible for the variable outcomes from the same therapy among patients. Tumour heterogeneity is now being explored by characterizing sub regions with distinct image characteristics, called habitats.[80] Based on spatial distributions of MR images and parametric maps, habitats of distinct physiologies such as viable cells, necrosis and edema could be delineated and provide unique information for therapeutic decision support. Spatial habitats derived from multi parametric MR data predicted 12-month survival for glioblastoma patients.[81] A processing pipeline for delineating tumour habitats from metabolic and physiological images that showed an association between the habitats and recurrence patterns on irradiated glioblastoma.[82]

Multiparametric images combine the information from different images, thus allowing improvement of characterization of complex tissue therapeutic responses. Radiomics refers to high-throughput extraction of quantitative features from multi sequence, multiparametric images that may aid in clinical decision making.[83] The features typically consist of intensity, shape and texture that capture tumour heterogeneities. Numerous radiomics studies have been published recently in cancer research including radiation treatment.[84] Texture analysis of DCE MRI identified tumour sub regions that predicted breast cancer response to neoadjuvant therapy.[85] A recent study showed that radiomics from T_2-weighted MR images achieved significantly higher performance than DWI for determining complete response of rectal cancer after chemo-radiation treatment.[86] Instead of using explicitly hand-crafted features in traditional radiomics studies, machine learning based methods generate radiomics features directly from neural network learning on a training dataset.[87] The features extracted by machine learning on multisequence MRIs of glioblastoma patients showed better performance for prediction of overall survival than traditional risk factors.[88] However, machine learning-based features may present barriers for understanding due to the complex modelling. Deep understanding of the method and prospective validation will be required to establish clinical utilities of the technique for cancer treatment.

QUALITY ASSURANCE

To date, a single standardized approach to quality assurance for both MR simulators and MRL does not exist. For MR scanners used for MR simulation early quality assurance efforts focused on the quantification of spatial distortion.[5] More recently Paulson et al[89] have described processes and procedures, including quality assurance, for MR simulation on a high field wide bore cylindrical (3 T, 70 cm diameter) MR system. While the report focuses on procedures unique to MR simulation for radiation therapy, many of the elements of this report were developed based on previously published quality assurance methods including work by the American Association of Physicists in Medicine (AAPM) MR Subcommittee (Task Group 1)[90] and the quality assurance program recommendations provided by the American College of Radiology MR accreditation program as discussed in several references.[91,92] To address the need for a standardized approach to quality assurance of MR simulators, the AAPM has recently formed Task Group number 284 (Magnetic Resonance Imaging Simulation in Radiotherapy: Considerations for Clinical Implementation, Optimization, and Quality Assurance) with the charge of providing guidance on facility design, siting, MR safety, RT-specific clinical workflows including acquisition protocols, distortion and motion management and finally the development of quality assurance protocols. While the report is not available at the time of publication of this article, it is expected that the finalized report will be available imminently to the general public. Similarly, a standardized, vendor neutral approach to quality assurance of MRLs does not exist at the time of publication. In response to this need both commercial and joint industry-academic efforts are currently underway. Phantoms for quality control of the MR component of the MRL are becoming commercially available (Modus QA, London ON, Canada) while an international consortium of users of the Elekta 1.5 T MRL system has been established to address the development and clinical translation of this system.[93] A major task of this group will be the development of all aspect of quality assurance including reference dosimetry, off line and real time treatment, end-to-end, patient and MR quality assurance. As MRL systems continue to translate into clinical practice, it is highly likely that vendor neutral protocols for MRL will be developed by professional societies such as the AAPM.

UNMET NEEDS AND OPPORTUNITIES

Much work remains to be done to ensure the successful integration and adaptation of both MR simulators and MRLs into the routine clinical workflow of radiation oncology departments. While many challenges remain, there also exists a unique opportunity which is to leverage the significant work and advances in the field of MR imaging already underway in the diagnostic MR imaging community and to translate and adapt these to the need of radiation oncology. This will require closer collaboration amongst clinicians and scientists from both radiology and radiation oncology necessitating the removal of preexisting silos that have developed over the past several decades. To this end, a recent editorial in a major scientific MR imaging journal has

identified this need and called for closer collaborations between both diagnostic and therapy scientists and clinicians. This is to not only expedite and translate advances developed for diagnostic MR applications to therapy but to also focus on therapy specific MR imaging challenges.[23] Fostering and developing collaborations across these disciplines will also require support from both national and international scientific and professional societies such as the AAPM, the RSNA, International Society of Magnetic Resonance in Medicine (ISMRM), American Society for Radiation Oncology (ASTRO), and the European Society for Radiation Oncology (ESTRO). To turn this vision into reality, the authors encourage communication at all levels starting with grass roots efforts to multi institutional formalized efforts such as working groups and conferences.

CONCLUSIONS AND FUTURE TRENDS

Since the early 1990's the use of MRI in radiation oncology has experienced rapid growth. With the introduction of integrated treatment system such as the MRL real time soft tissue visualization, motion managements and dose delivery during treatment is now possible. The authors of this report therefore conclude that MRI in radiation therapy has a bright future and will enable the field to advance to a higher level of patient care and in doing so produce improved treatment outcomes.

While the authors have attempted to highlight the importance and value of MR in radiation therapy, debate continues regarding its role and efficacy[94,95] What is clear is that the soft tissue contrast and ability to visualize *in vivo* organ motion afforded by MR when integrated into a single hybrid imaging and treatment system will have significant advantage as shown by Pollard et al.[56] Solutions to technical difficulties such as distortion, creation of sCT, ERE, and heating effect will no doubt be resolved or mitigated by ongoing research and development. Staffing and training are another issues that respective societies need to look at carefully and provide guidelines. Since 1990, diagnostic and therapeutic divisions of Radiology have formed their own individual departments with little or no interactions. Imaging based radiation treatment is bringing both teams together. However training and expertise still remain independent across departments and institutions. There is an urgent need to integrate imaging components in radiation treatments and hence both groups have to share some responsibility for these developments and knowledge sharing if the integrated devices are to become successful. Finally, MRI-based systems have to provide clinical data showing superiority over traditional treatment. Preliminary outcome studies from these integrated devices are encouraging.[96]

With introduction of proton beam radiation therapy,[97] a new sense of confidence in improved patient care exists. With advances in MRI and speculation exists regarding the integration of these two systems, Raaymakers et al[98] provided a feasibility of its use. Additionally more work has been reported on simulation and real testing of MRI and proton beam.[99] It is expected that the success of the MRL will soon translate into MRI-proton units thus compounding the benefit of MRI and Protons. The image quality of MRL with same magnetic fields are identical to that of the diagnostic MRI units thus eliminating the fear of distortion, scatter and leakage as shown by Wang et al.[91]

It is our conclusion that the use of MRI in radiation oncology is paving the way for improved patient care that may translate into actual improved outcomes. Many technical hurdles are being investigated with academic institutions and vendors for an integrated and seamless process.

REFERENCES

1. Citrin DE. Recent developments in radiotherapy. *N Engl J Med Overseas Ed* 2017; **377**: 1065–75. doi: https://doi.org/10.1056/NEJMra1608986
2. Srivastava SP, Cheng C-W, Das IJ. Image guidance-based target volume margin expansion in IMRT of head and neck cancer. *Technol Cancer Res Treat* 2016; **15**: 107–13. doi: https://doi.org/10.1177/1533034614561162
3. Martinez AA, Yan D, Lockman D, Brabbins D, Kota K, Sharpe M, et al. Improvement in dose escalation using the process of adaptive radiotherapy combined with three-dimensional conformal or intensity-modulated beams for prostate cancer. *Int J Radiat Oncol Biol Phys* 2001; **50**: 1226–34. doi: https://doi.org/10.1016/S0360-3016(01)01552-8
4. Das IJ, Cheng CW, Cao M, Johnstone PA. Computed tomography imaging parameters for inhomogeneity correction in radiation treatment planning. *J Med Phys* 2016; **41**: 3–11. doi: https://doi.org/10.4103/0971-6203.177277
5. Mah D, Steckner M, Palacio E, Mitra R, Richardson T, Hanks GE. Characteristics and quality assurance of a dedicated open 0.23 T MRI for radiation therapy simulation. *Med Phys* 2002; **29**: 2541–7. doi: https://doi.org/10.1118/1.1513991
6. Glide-Hurst CK, Wen N, Hearshen D, Kim J, Pantelic M, Zhao B, et al. Initial clinical experience with a radiation oncology dedicated open 1.0T MR-simulation. *J Appl Clin Med Phys* 2015; **16**: 218–40. doi: https://doi.org/10.1120/jacmp.v16i2.5201
7. Hsu S-H, Cao Y, Huang K, Feng M, Balter JM. Investigation of a method for generating synthetic CT models from MRI scans of the head and neck for radiation therapy. *Phys Med Biol* 2013; **58**: 8419–35. doi: https://doi.org/10.1088/0031-9155/58/23/8419
8. Tyagi N, Fontenla S, Zhang J, Cloutier M, Kadbi M, Mechalakos J, et al. Dosimetric and workflow evaluation of first commercial synthetic CT software for clinical use in pelvis. *Phys Med Biol* 2017; **62**: 2961–75. doi: https://doi.org/10.1088/1361-6560/aa5452
9. Han X. MR-based synthetic CT generation using a deep convolutional neural network method. *Med Phys* 2017; **44**: 1408–19. doi: https://doi.org/10.1002/mp.12155
10. Wang H, Chandarana H, Block KT, Vahle T, Fenchel M, Das IJ. Dosimetric evaluation of synthetic CT for magnetic resonance-only based radiotherapy planning of lung cancer. *Radiat Oncol* 2017; **12**: 108. doi: https://doi.org/10.1186/s13014-017-0845-5
11. Wang H, Du K, Qu J, Chandarana H, Das IJ. Dosimetric evaluation of magnetic resonance-generated synthetic CT for

radiation treatment of rectal cancer. *PLoS One* 2018; **13**: e0190883. doi: https://doi.org/10.1371/journal.pone.0190883
12. Chandarana H, Wang H, Tijssen RHN, Das IJ.;in press Emerging role of MRI in radiation therapy. *J Mag Res Imag* **375**. doi: https://doi.org/10.1002/jmri.26271
13. Jaffray DA, Carlone MC, Milosevic MF, Breen SL, Stanescu T, Rink A, et al. A facility for magnetic resonance–guided radiation therapy. *Semin Radiat Oncol* 2014; **24**: 193–5. doi: https://doi.org/10.1016/j.semradonc.2014.02.012
14. Lagendijk JJW, Raaymakers BW, Raaijmakers AJE, Overweg J, Brown KJ, Kerkhof EM, et al. MRI/linac integration. *Radiotherapy and Oncology* 2008; **86**: 25–9. doi: https://doi.org/10.1016/j.radonc.2007.10.034
15. Mutic S, Dempsey JF. The viewray system: magnetic resonance–guided and controlled radiotherapy. *Semin Radiat Oncol* 2014; **24**: 196–9. doi: https://doi.org/10.1016/j.semradonc.2014.02.008
16. Acharya S, Fischer-Valuck BW, Kashani R, Parikh P, Yang D, Zhao T, et al. Online magnetic resonance image guided adaptive radiation therapy: First clinical applications. *Int J Radiat Oncol Biol Phys* 2016; **94**: 394–403. doi: https://doi.org/10.1016/j.ijrobp.2015.10.015
17. Lagendijk JJW, Raaymakers BW, Van den Berg CAT, Moerland MA, Philippens ME, van Vulpen M. MR guidance in radiotherapy. *Phys Med Biol* 2014; **59**: R349–R369. doi: https://doi.org/10.1088/0031-9155/59/21/R349
18. Keall PJ, Barton M, Crozier S. The australian magnetic resonance imaging–linac program. *Semin Radiat Oncol* 2014; **24**: 203–6. doi: https://doi.org/10.1016/j.semradonc.2014.02.015
19. Fallone BG. The rotating biplanar linac–magnetic resonance imaging system. *Semin Radiat Oncol* 2014; **24**: 200–2. doi: https://doi.org/10.1016/j.semradonc.2014.02.011
20. Fallone BG, Murray B, Rathee S, Stanescu T, Steciw S, Vidakovic S, et al. First MR images obtained during megavoltage photon irradiation from a prototype integrated linac-MR system. *Med Phys* 2009; **36**(6Part1): 2084–8. doi: https://doi.org/10.1118/1.3125662
21. Raaymakers BW, de Boer JCJ, Knox C, Crijns SPM, Smit K, Stam MK, et al. Integrated megavoltage portal imaging with a 1.5 T MRI linac. *Phys Med Biol* 2011; **56**: N207–N214. doi: https://doi.org/10.1088/0031-9155/56/19/N01
22. Mizowaki T, Nagata Y, Okajima K, Murata R, Yamamoto M, Kokubo M, et al. Development of an MR simulator: experimental verification of geometric distortion and clinical application. *Radiology* 1996; **199**: 855–60. doi: https://doi.org/10.1148/radiology.199.3.8638017
23. McGee KP, Hu Y, Tryggestad E, Brinkmann D, Witte B, Welker K, et al. MRI in radiation oncology: Underserved needs. *Magn Reson Med* 2016; **75**: 11–14. doi: https://doi.org/10.1002/mrm.25826
24. Schmidt MA, Payne GS. Radiotherapy planning using MRI. *Phys Med Biol* 2015; **60**: R323–R361. doi: https://doi.org/10.1088/0031-9155/60/22/R323
25. McGee KP, Stormont RS, Lindsay SA, Taracila V, Savitskij D, Robb F, et al. Characterization and evaluation of a flexible MRI receive coil array for radiation therapy MR treatment planning using highly decoupled RF circuits. *Phys Med Biol* 2018; **63**: 08NT02. doi: https://doi.org/10.1088/1361-6560/aab691
26. Mizowaki T, Nagata Y, Okajima K, Kokubo M, Negoro Y, Araki N, et al. Reproducibility of geometric distortion in magnetic resonance imaging based on phantom studies. *Radiotherapy and Oncology* 2000; **57**: 237–42. doi: https://doi.org/10.1016/S0167-8140(00)00234-6
27. Weygand J, Fuller CD, Ibbott GS, Mohamed ASR, Ding Y, Yang J, et al. Spatial precision in magnetic resonance imaging–guided radiation therapy: The role of-geometric distortion. *Int J Radiat Oncol Biol Phys* 2016; **95**: 1304–16. doi: https://doi.org/10.1016/j.ijrobp.2016.02.059
28. Weavers PT, Tao S, Trzasko JD, Shu Y, Tryggestad EJ, Gunter JL, et al. Image-based gradient non-linearity characterization to determine higher-order spherical harmonic coefficients for improved spatial position accuracy in magnetic resonance imaging. *Magn Reson Imaging* 2017; **38**: 54–62. doi: https://doi.org/10.1016/j.mri.2016.12.020
29. Schenck JF. The role of magnetic susceptibility in magnetic resonance imaging: MRI magnetic compatibility of the first and second kinds. *Med Phys* 1996; **23**: 815–50. doi: https://doi.org/10.1118/1.597854
30. Bernstein MA, King KF, Zhou XJ. *Handbook of MRI pulse sequences*. Cambridge, MA: Elsevier Academic Press; 2004.
31. Reynolds M, Fallone BG, Rathee S. Dose response of selected solid state detectors in applied homogeneous transverse and longitudinal magnetic fields. *Med Phys* 2014; **41**: 092103. doi: https://doi.org/10.1118/1.4893276
32. Rasch C, Keus R, Pameijer FA, Koops W, de Ru V, Muller S, et al. The potential impact of CT-MRI matching on tumor volume delineation in advanced head and neck cancer. *Int J Radiat Oncol Biol Phys* 1997; **39**: 841–8. doi: https://doi.org/10.1016/S0360-3016(97)00465-3
33. Fiorino C, Reni M, Bolognesi A, Cattaneo GM, Calandrino R. Intra- and inter-observer variability in contouring prostate and seminal vesicles: implications for conformal treatment planning. *Radiother Oncol* 1998; **47**: 285–92. doi: https://doi.org/10.1016/S0167-8140(98)00021-8
34. Geets X, Daisne JF, Arcangeli S, Coche E, De Poel M, Duprez T, et al. Inter-observer variability in the delineation of pharyngo-laryngeal tumor, parotid glands and cervical spinal cord: comparison between CT-scan and MRI. *Radiother Oncol* 2005; **77**: 25–31. doi: https://doi.org/10.1016/j.radonc.2005.04.010
35. Nijkamp J, de Haas-Kock DF, Beukema JC, Neelis KJ, Woutersen D, Ceha H, et al. Target volume delineation variation in radiotherapy for early stage rectal cancer in the Netherlands. *Radiother Oncol* 2012; **102**: 14–21. doi: https://doi.org/10.1016/j.radonc.2011.08.011
36. Louie AV, Rodrigues G, Olsthoorn J, Palma D, Yu E, Yaremko B, et al. Inter-observer and intra-observer reliability for lung cancer target volume delineation in the 4D-CT era. *Radiother Oncol* 2010; **95**: 166–71. doi: https://doi.org/10.1016/j.radonc.2009.12.028
37. Van de Steene J, Linthout N, de Mey J, Vinh-Hung V, Claassens C, Noppen M, et al. Definition of gross tumor volume in lung cancer: inter-observer variability. *Radiother Oncol* 2002; **62**: 37–49. doi: https://doi.org/10.1016/S0167-8140(01)00453-4
38. Weltens C, Menten J, Feron M, Bellon E, Demaerel P, Maes F, et al. Interobserver variations in gross tumor volume delineation of brain tumors on computed tomography and impact of magnetic resonance imaging. *Radiother Oncol* 2001; **60**: 49–59. doi: https://doi.org/10.1016/S0167-8140(01)00371-1
39. Ramsey CR, Oliver AL. Magnetic resonance imaging based digitally reconstructed radiographs, virtual simulation, and three-dimensional treatment planning for brain neoplasms. *Med Phys* 1998; **25**: 1928–34. doi: https://doi.org/10.1118/1.598382
40. Kagawa K, Lee WR, Schultheiss TE, Hunt MA, Shaer AH, Hanks GE. Initial clinical assessment of CT-MRI image fusion software in localization of the prostate for 3D conformal radiation therapy. *Int J Radiat Oncol Biol Phys* 1997; **38**: 319–25. doi: https://doi.org/10.1016/S0360-3016(96)00620-7
41. Kemppainen R, Vaara T, Joensuu T, Kiljunen T. Accuracy and precision of patient

positioning for pelvic MR-only radiation therapy using digitally reconstructed radiographs. *Phys Med Biol* 2018; **63**: 055009. doi: https://doi.org/10.1088/1361-6560/aaad21
42. Johnstone E, Wyatt JJ, Henry AM, Short SC, Sebag-Montefiore D, Murray L, et al. Systematic review of synthetic computed tomography generation methodologies for use in magnetic resonance imaging–only radiation therapy. *Int J Radiat Oncol Biol Phys* 2018; **100**: 199–217. doi: https://doi.org/10.1016/j.ijrobp.2017.08.043
43. Jonsson JH, Johansson A, Söderström K, Asklund T, Nyholm T. Treatment planning of intracranial targets on MRI derived substitute CT data. *Radiother Oncol* 2013; **108**: 118–22. doi: https://doi.org/10.1016/j.radonc.2013.04.028
44. Korsholm ME, Waring LW, Edmund JM. A criterion for the reliable use of MRI-only radiotherapy. *Radiat Oncol* 2014; **9**: 16. doi: https://doi.org/10.1186/1748-717X-9-16
45. Lambert J, Greer PB, Menk F, Patterson J, Parker J, Dahl K, et al. MRI-guided prostate radiation therapy planning: Investigation of dosimetric accuracy of MRI-based dose planning. *Radiother Oncol* 2011; **98**: 330–4. doi: https://doi.org/10.1016/j.radonc.2011.01.012
46. Prior P, Chen X, Botros M, Paulson ES, Lawton C, Erickson B, et al. MRI-based IMRT planning for MR-linac: comparison between CT- and MRI-based plans for pancreatic and prostate cancers. *Phys Med Biol* 2016; **61**: 3819–42. doi: https://doi.org/10.1088/0031-9155/61/10/3819
47. Uh J, Merchant TE, Li Y, Li X, Hua C. MRI-based treatment planning with pseudo CT generated through atlas registration. *Med Phys* 2014; **41**: 051711. doi: https://doi.org/10.1118/1.4873315
48. Farjam R, Tyagi N, Veeraraghavan H, Apte A, Zakian K, Hunt MA, et al. Multiatlas approach with local registration goodness weighting for MRI-based electron density mapping of head and neck anatomy. *Med Phys* 2017; **44**: 3706–17. doi: https://doi.org/10.1002/mp.12303
49. Siversson C, Nordström F, Nilsson T, Nyholm T, Jonsson J, Gunnlaugsson A, et al. Technical Note: MRI only prostate radiotherapy planning using the statistical decomposition algorithm. *Med Phys* 2015; **42**: 6090–7. doi: https://doi.org/10.1118/1.4931417
50. Maspero M, Savenije MHF, Dinkla AM, Seevinck PR, Intven MPW, Jurgenliemk-Schulz IM. Dose evaluation of fast synthetic-CT generationusing a generative adversarial network for generalpelvis MR-only radiotherapy. *Phys Med Biol* **63**: 185001-13.
51. Wolterink JM, Dinkla AM, Savenije MHF, Seevinck PR, van den Berg CAT, Išgum I. Deep MR to CT Synthesis Using Unpaired Data. In: *Simulation and Synthesis in Medical Imaging; 2017*. Cham: Springer International Publishing; 2017.
52. Tyagi N, Fontenla S, Zelefsky M, Chong-Ton M, Ostergren K, Shah N, et al. Clinical workflow for MR-only simulation and planning in prostate. *Radiat Oncol* 2017; **12**: 119. doi: https://doi.org/10.1186/s13014-017-0854-4
53. Persson E, Gustafsson C, Nordström F, Sohlin M, Gunnlaugsson A, Petruson K, et al. MR-OPERA: A multicenter/multivendor validation of magnetic resonance imaging–only prostate treatment planning using synthetic computed tomography images. *Int J Radiat Oncol Biol Phys* 2017; **99**: 692–700. doi: https://doi.org/10.1016/j.ijrobp.2017.06.006
54. Balter JM, Haffty BG, Dunnick NR, Siegel EL. Imaging opportunities workshop P. imaging opportunities in radiation oncology. *Int J Radiat Oncol Biol Phys* 2011; **79**: 342–7.
55. U. Kishan A, Lee P. MRI-guided radiotherapy: Opening our eyes to the future. *Integr Cancer Sci Ther* 2016; **3**: 420–7. doi: https://doi.org/10.15761/ICST.1000181
56. Pollard JM, Wen Z, Sadagopan R, Wang J, Ibbott GS. The future of image-guided radiotherapy will be MR guided. *Br J Radiol* 2017; **90**: 20160667. doi: https://doi.org/10.1259/bjr.20160667
57. Lagendijk JJW, Raaymakers BW, van Vulpen M. The magnetic resonance imaging–linac system. *Semin Radiat Oncol* 2014; **24**: 207–9. doi: https://doi.org/10.1016/j.semradonc.2014.02.009
58. Raaymakers BW, Lagendijk JJ, Overweg J, Kok JG, Raaijmakers AJ, Kerkhof EM, et al. Integrating a 1.5 T MRI scanner with a 6 MV accelerator: proof of concept. *Phys Med Biol* 2009; **54**: N229–N237. doi: https://doi.org/10.1088/0031-9155/54/12/N01
59. Ouyang FS, Guo BL, Zhang B, Dong YH, Zhang L, Mo XK, et al. Exploration and validation of radiomics signature as an independent prognostic biomarker in stage III-IVb nasopharyngeal carcinoma. *Oncotarget* 2017; **8**: 74869–79. doi: https://doi.org/10.18632/oncotarget.20423
60. Cao Y. The promise of dynamic contrast-enhanced imaging in radiation therapy. *Semin Radiat Oncol* 2011; **21**: 147–56. doi: https://doi.org/10.1016/j.semradonc.2010.11.001
61. Cao Y, Popovtzer A, Li D, Chepeha DB, Moyer JS, Prince ME, et al. Early prediction of outcome in advanced head-and-neck cancer based on tumor blood volume alterations during therapy: a prospective study. *Int J Radiat Oncol Biol Phys* 2008; **72**: 1287–90. doi: https://doi.org/10.1016/j.ijrobp.2008.08.024
62. Wang C-H, Yin FF, Horton J, Chang Z. Review of treatment assessment using DCE-MRI in breast cancer radiation therapy. *World J Methodol* 2014; **4**: 46–58. doi: https://doi.org/10.5662/wjm.v4.i2.46
63. Wang H, Farjam R, Feng M, Hussain H, Ten Haken RK, Lawrence TS, et al. Arterial perfusion imaging–defined subvolume of intrahepatic cancer. *Int J Radiat Oncol Biol Phys* 2014; **89**: 167–74. doi: https://doi.org/10.1016/j.ijrobp.2014.01.040
64. George ML, Dzik-Jurasz ASK, Padhani AR, Brown G, Tait DM, Eccles SA, et al. Non-invasive methods of assessing angiogenesis and their value in predicting response to treatment in colorectal cancer. *Br J Surg* 2001; **88**: 1628–36. doi: https://doi.org/10.1046/j.0007-1323.2001.01947.x
65. Zahra MA, Tan LT, Priest AN, Graves MJ, Arends M, Crawford RAF, et al. Semiquantitative and quantitative dynamic contrast-enhanced magnetic resonance imaging measurements predict radiation response in cervix cancer. *Int J Radiat Oncol Biol Phys* 2009; **74**: 766–73. doi: https://doi.org/10.1016/j.ijrobp.2008.08.023
66. Tao X, Wang L, Hui Z, Liu L, Ye F, Song Y, et al. DCE-MRI perfusion and permeability parameters as predictors of tumor response to CCRT in patients with locally advanced NSCLC. *Sci Rep* 2016; **6**: 35569. doi: https://doi.org/10.1038/srep35569
67. Bisdas S, Naegele T, Ritz R, Dimostheni A, Pfannenberg C, Reimold M, et al. Distinguishing recurrent high-grade gliomas from radiation injury: a pilot study using dynamic contrast-enhanced MR imaging. *Acad Radiol* 2011; **18**: 575–83.
68. Thoeny HC, Ross BD. Predicting and monitoring cancer treatment response with diffusion-weighted MRI. *J Magn Reson Imaging* 2010; **32**: 2–16. doi: https://doi.org/10.1002/jmri.22167
69. Farjam R, Tsien CI, Feng FY, Gomez-Hassan D, Hayman JA, Lawrence TS, et al. Investigation of the diffusion abnormality index as a new imaging biomarker for early assessment of brain tumor response to radiation therapy. *Neuro Oncol* 2014; **16**: 131–9. doi: https://doi.org/10.1093/neuonc/not153
70. Pramanik PP, Parmar HA, Mammoser AG, Junck LR, Kim MM, Tsien CI, et al. Hypercellularity components of glioblastoma identified by high b-value diffusion-weighted

imaging. *Int J Radiat Oncol Biol Phys* 2015; **92**: 811–9. doi: https://doi.org/10.1016/j.ijrobp.2015.02.058

71. Galbán CJ, Mukherji SK, Chenevert TL, Meyer CR, Hamstra DA, Bland PH, et al. A feasibility study of parametric response map analysis of diffusion-weighted magnetic resonance imaging scans of head and neck cancer patients for providing early detection of therapeutic efficacy. *Transl Oncol* 2009; **2**: 184–90. doi: https://doi.org/10.1593/tlo.09175
72. liu L, Wu N, Ouyang H, Dai J-R, Wang W-H. Diffusion-weighted MRI in early assessment of tumour response to radiotherapy in high-risk prostate cancer. *Br J Radiol* 2014; **87**: 20140359. doi: https://doi.org/10.1259/bjr.20140359
73. Cao Y, Tsien CI, Sundgren PC, Nagesh V, Normolle D, Buchtel H, et al. Dynamic contrast-enhanced magnetic resonance imaging as a biomarker for prediction of radiation-induced neurocognitive dysfunction. *Clin Cancer Res* 2009; **15**: 1747–54. doi: https://doi.org/10.1158/1078-0432.CCR-08-1420
74. Chapman CH, Zhu T, Nazem-Zadeh M, Tao Y, Buchtel HA, Tsien CI, et al. Diffusion tensor imaging predicts cognitive function change following partial brain radiotherapy for low-grade and benign tumors. *Radiother Oncol* 2016; **120**: 234–40. doi: https://doi.org/10.1016/j.radonc.2016.06.021
75. Zhu T, Chapman CH, Tsien C, Kim M, Spratt DE, Lawrence TS, et al. Effect of the maximum dose on white matter fiber bundles using longitudinal diffusion tensor imaging. *Int J Radiat Oncol Biol Phys* 2016; **96**: 696–705. doi: https://doi.org/10.1016/j.ijrobp.2016.07.010
76. Nazem-Zadeh M-R, Chapman CH, Chenevert T, Lawrence TS, Ten Haken RK, Tsien CI, et al. Response-driven imaging biomarkers for predicting radiation necrosis of the brain. *Phys Med Biol* 2014; **59**: 2535–47. doi: https://doi.org/10.1088/0031-9155/59/10/2535
77. Cao Y, Wang H, Johnson TD, Pan C, Hussain H, Balter JM, et al. Prediction of liver function by using magnetic resonance-based portal venous perfusion imaging. *Int J Radiat Oncol Biol Phys* 2013; **85**: 258–63. doi: https://doi.org/10.1016/j.ijrobp.2012.02.037
78. Wang H, Feng M, Jackson A, Ten Haken RK, Lawrence TS, Cao Y. Local and global function model of the liver. *Int J Radiat Oncol Biol Phys* 2016; **94**: 181–8. doi: https://doi.org/10.1016/j.ijrobp.2015.09.044
79. El Naqa I, Johansson A, Owen D, Cuneo K, Cao Y, Matuszak M, et al. Modeling of normal tissue complications using imaging and biomarkers after radiation therapy for hepatocellular carcinoma. *Int J Radiat Oncol Biol Phys* 2018; **100**: 335–43. doi: https://doi.org/10.1016/j.ijrobp.2017.10.005
80. Chang Y-CC, Ackerstaff E, Tschudi Y, Jimenez B, Foltz W, Fisher C, et al. Delineation of tumor habitats based on dynamic contrast enhanced MRI. *Sci Rep* 2017; **7**: 9746. doi: https://doi.org/10.1038/s41598-017-09932-5
81. Lee J, Narang S, Martinez JJ, Rao G, Rao A. Associating spatial diversity features of radiologically defined tumor habitats with epidermal growth factor receptor driver status and 12-month survival in glioblastoma: methods and preliminary investigation. *J Med Imaging* 2015; **2**: 041006. doi: https://doi.org/10.1117/1.JMI.2.4.041006
82. You D, Kim MM, Aryal MP, Parmar H, Piert M, Lawrence TS, et al. Tumor image signatures and habitats: a processing pipeline of multimodality metabolic and physiological images. *J Med Imaging* 2018; **5**: 011009.
83. Aerts HJWL, Velazquez ER, Leijenaar RTH, Parmar C, Grossmann P, Carvalho S, et al. Decoding tumour phenotype by noninvasive imaging using a quantitative radiomics approach. *Nat Commun* 2014; **5**: 4006. doi: https://doi.org/10.1038/ncomms5006
84. Gillies RJ, Kinahan PE, Hricak H. Radiomics: images are more than pictures, they are data. *Radiology* 2016; **278**: 563–77. doi: https://doi.org/10.1148/radiol.2015151169
85. Wu J, Gong G, Cui Y, Li R. Intratumor partitioning and texture analysis of dynamic contrast-enhanced (DCE)-MRI identifies relevant tumor subregions to predict pathological response of breast cancer to neoadjuvant chemotherapy. *J Magn Reson Imag* 2016; **44**: 1107–15. doi: https://doi.org/10.1002/jmri.25279
86. Horvat N, Veeraraghavan H, Khan M, Blazic I, Zheng J, Capanu M, et al. MR imaging of rectal cancer: Radiomics analysis to assess treatment response after neoadjuvant therapy. *Radiology* 2018; **287**: 833–43. doi: https://doi.org/10.1148/radiol.2018172300
87. Parmar C, Grossmann P, Bussink J, Lambin P, Aerts HJWL. Machine learning methods for quantitative radiomic biomarkers. *Sci Rep* 2015; **5**: 13087. doi: https://doi.org/10.1038/srep13087
88. Lao J, Chen Y, Li Z-C, Li Q, Zhang J, Liu J, et al. A Deep learning-based radiomics model for prediction of survival in glioblastoma multiforme. *Sci Rep* 2017; **7**: 10353. doi: https://doi.org/10.1038/s41598-017-10649-8
89. Paulson ES, Erickson B, Schultz C, Allen Li X, Li A X. Comprehensive MRI simulation methodology using a dedicated MRI scanner in radiation oncology for external beam radiation treatment planning. *Med Phys* 2015; **42**: 28–39. doi: https://doi.org/10.1118/1.4896096
90. Jackson EF, Bronskill MJ, Drost DJ, Och J, Pooley RA, Sobol WT. *AcceptanceTesting and Quality Assurance Procedures for Magnetic Resonance Imaging Facilities*. College Park, MD: American Association of Physicists in Medicine; 2010.
91. Wang J, Yung J, Kadbi M, Hwang K, Ding Y, Ibbott GS. Assessment of image quality and scatter and leakage radiation of an integrated MR-LINAC system. *Med Phys* 2018; **45**: 1204–9. doi: https://doi.org/10.1002/mp.12767
92. DeMartini WB, Rahbar H. Breast magnetic resonance imaging technique at 1.5 T and 3 T: requirements for quality imaging and American College of Radiology accreditation. *Magn Reson Imaging Clin N Am* 2013; **21**: 475–82.
93. Kerkmeijer LGW, Fuller CD, Verkooijen HM, Verheij M, Choudhury A, Harrington KJ, et al. The MRI-linear accelerator consortium: evidence-based clinical introduction of an innovation in radiation oncology connecting researchers, methodology, data collection, quality assurance, and technical development. *Front Oncol* 2016; **6**: 215. doi: https://doi.org/10.3389/fonc.2016.00215
94. Glide-Hurst CK, Low DA, Orton CG. Point/Counterpoint. MRI/CT is the future of radiotherapy treatment planning. *Med Phys* 2014; **41**: 110601. doi: https://doi.org/10.1118/1.4894495
95. Cao M, Padgett KR, Rong Y. Are in-house diagnostic MR physicists necessary for clinical implementation of MRI guided radiotherapy? *J Appl Clin Med Phys* 2017; **18**: 6–9. doi: https://doi.org/10.1002/acm2.12171
96. Rudra S, Jiang N, Rosenberg SA, Olsen JR, Parikh PJ, Bassetti MF, et al. High dose adaptive MRI guided radiation therapy improves overall survival of inoperable pancreatic cancer. *Int J Radiat Oncol Biol Phys* 2017; **99**: E184. doi: https://doi.org/10.1016/j.ijrobp.2017.06.1042
97. Das IJ, Paganetti H. eds. *Principle and practice of proton beam therapy*. Madison, WI: Medical Physics Publishing Inc; 2015.
98. Raaymakers BW, Raaijmakers AJE, Lagendijk JJW. Feasibility of MRI guided proton therapy: magnetic field dose effects. *Phys Med Biol* 2008; **53**: 5615–22. doi: https://doi.org/10.1088/0031-9155/53/20/003
99. Oborn BM, Dowdell S, Metcalfe PE, Crozier S, Mohan R, Keall PJ. Proton beam deflection in MRI fields: Implications for MRI-guided proton therapy. *Med Phys* 2015; **42**: 2113–24. doi: https://doi.org/10.1118/1.4916661